Article

Chemistry & Biology

Tamoxifen Inhibits CDK5 Kinase Activity by Interacting with p35/p25 and Modulates the Pattern of Tau Phosphorylation

Graphical Abstract

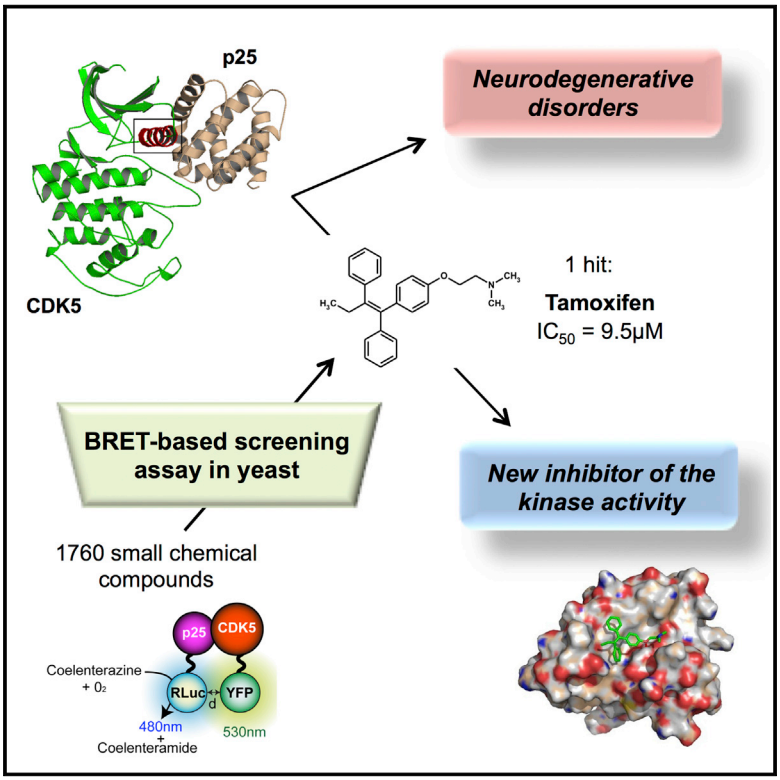

Highlights

- The CDK5/p25 interaction is related to neurodegenerative diseases
- Tamoxifen, an antitumor agent, inhibits CDK5/p25 activity
- Tamoxifen acts by binding on p25
- Tamoxifen can be used for further development of therapeutic drugs

Authors

Caroline Corbel, Bing Zhang, ..., Véronique Le Tilly, Stéphane Bach

Correspondence

bach@sb-roscoff.fr

In Brief

Corbel et al. describe the discovery of a new target for the widely used drug tamoxifen: the CDK5/p25 interaction. Treatment of primary neurons with tamoxifen results in decreased phosphorylated forms of tau, one of the neuropathological hallmarks of Alzheimer's disease.

Corbel et al., 2015, Chemistry & Biology 22, 472–482
April 23, 2015
http://dx.doi.org/10.1016/j.chembiol.2015.03.009

CellPress

Chemistry & Biology
Article

Tamoxifen Inhibits CDK5 Kinase Activity by Interacting with p35/p25 and Modulates the Pattern of Tau Phosphorylation

Caroline Corbel,[1,2,3] Bing Zhang,[4] Annabelle Le Parc,[2] Blandine Baratte,[1] Pierre Colas,[1] Cyril Couturier,[5] Kenneth S. Kosik,[3] Isabelle Landrieu,[6,7] Véronique Le Tilly,[2] and Stéphane Bach[1,*]

[1]USR3151-CNRS/UPMC, Protein Phosphorylation and Disease Laboratory, Station Biologique de Roscoff, CS 90074, 29688 Roscoff, Bretagne, France

[2]EA4250-LIMATB-EG2B, Centre de Recherche et d'Enseignement Yves Coppens, Université de Bretagne Sud, 56017 Vannes, France

[3]Kosik Laboratory, Neuroscience Research Institute, Department of Molecular, Cellular and Developmental Biology, University of California, Santa Barbara, CA 93106, USA

[4]School of Renewable Energy, North China Electric Power Electricity, 071003 Beijing, China

[5]UMR761-INSERM Lille University, Biostructures and Drug Discovery, 59006 Lille, France

[6]UMR8576 CNRS-Lille North of France University, 59658 Villeneuve d'Ascq, France

[7]Interdisciplinary Research Institute (IRI), 58658 Villeneuve d'Ascq, France

*Correspondence: bach@sb-roscoff.fr

http://dx.doi.org/10.1016/j.chembiol.2015.03.009

SUMMARY

Cyclin-dependent kinase 5 (CDK5) is a multifunctional enzyme that plays numerous roles, notably in brain development. CDK5 is activated through its association with the activators, p35 and p39, rather than by cyclins. Proteolytic procession of the N-terminal part of its activators has been linked to Alzheimer's disease and various other neuropathies. The interaction with the proteolytic product p25 prolongs CDK5 activation and modifies the substrate specificity. In order to discover small-molecule inhibitors of the interaction between CDK5 and p25, we have used a bioluminescence resonance energy transfer (BRET)-based screening assay. Among the 1,760 compounds screened, the generic drug tamoxifen has been identified. The inhibition of the CDK5 activity by tamoxifen was notably validated by monitoring the phosphorylation state of tau protein. The study of the molecular mechanism of inhibition indicates that tamoxifen interacts with p25 to block the CDK5/p25 interaction and pave the way for new treatments of tauopathies.

INTRODUCTION

More than 35 million people are estimated to be living with dementia worldwide. By 2015, this number is projected to reach 115+ million (Feldman et al., 2014). This corresponds to the current population of France and Spain. For the World Health Organization, it represents a public health priority. Among neurodegenerative dementias, the most common is Alzheimer's disease (AD). Neuropathological hallmarks for AD are: (1) extensive cell death; (2) extracellular deposits of amyloid (neuritic) plaques composed of β-amyloid (Aβ) peptides; (3) intraneuronal aggregates of hyperphosphorylated tau, a microtubule-associated protein (Cruz and Tsai, 2004). The first description was presented in 1906 by Dr. Alois Alzheimer on the brain of his patient, Auguste Deter. Despite over a century of extensive research (5,000 research articles related to AD per year on PubMed) and the massive impact on our societies, effective treatments remain to be discovered. Current therapies (e.g. based on cholinesterase inhibition) are only symptomatic with a modest effect (Feldman et al., 2014). Therapeutic strategies directed toward the molecular bases of AD include the inhibition of tau hyperphosphorylation because it has been shown that tau pathology is related to neuronal loss (Cohen et al., 2013). One of the major tau kinases is cyclin-dependent kinase 5 (CDK5), a member of the serine/threonine kinase family of cyclin-dependent kinases.

Contrary to most CDKs that are implicated in the regulation of the cell division cycle, CDK5 plays a crucial role during the development of the CNS, notably by regulating neuronal migration (Malumbres and Barbacid, 2005; Smith et al., 2001). Disruption of the *CDK5* locus in mice results in lesions in the CNS associated with perinatal mortality (Ohshima et al., 1996). CDK5 is a catalytic subunit that has no enzymatic activity as a monomer. It is activated by binding to its activating subunits, p35 or p39, which are structurally related to cyclins (activators of cell-cycle CDKs) but display no homology at the amino acid level with these activators (Tarricone et al., 2001). In contrast to the other CDKs, full CDK5 activation does not require phosphorylation of the activation loop (Dhavan and Tsai, 2001). Studies have shown that neurotoxicity induces proteolytic cleavage of the p35 subunit by calcium-regulated calpains (Lee et al., 2000). The binding of CDK5 to the N-terminal truncated product p25, so-called neurotoxic activator, stabilizes the active dimer, changes the cellular location, and alters its substrate specificity promoting neurodegeneration (Patrick et al., 1999). In vitro experiments have shown that the conversion of p35 to p25 does not change significantly the steady-state kinetic parameters of tau or histone H1 phosphorylation by CDK5 (Peterson et al., 2010).

CDK5 is ubiquitously expressed but its activity is restricted to tissues expressing its regulators p35/p39 and their truncated

versions. Originally considered as a brain kinase, CDK5 kinase activity is not restricted to post-mitotic neurons and was notably observed in various pancreatic cancer cell lines (Feldmann et al., 2010; Lew et al., 1992), invasive breast cancer cells (Goodyear and Sharma, 2007), and others (for review see Contreras-Vallejos et al., 2012).

In view of these implications of CDK5 kinase activity in both neurodegenerative disease and cancer, two of the most important diseases in the 21st century, CDK5 is an attractive target to discover new therapeutic treatments. Small molecular weight inhibitors of CDK5 have been described, including roscovitine, diaminothiazoles, aloisines, and indirubines (Laha et al., 2011; Meijer et al., 1997; Mettey et al., 2003; Polychronopoulos et al., 2004). Co-crystallization experiments have shown that these inhibitors act by direct competition with ATP for binding to the catalytic cleft. This is also the case for almost all kinase inhibitors on the market (Bharate et al., 2013). Target selectivity remains a formidable challenge in drug development to tackle the appearance of deleterious side effects during treatment. This first generation of inhibitors might, in principle, be able to interact in vivo with some of the 2,000 ATP-utilizing enzymes present in the human proteome, including 518+ kinases, and with the numerous other nucleotide-binding proteins (for review see Guiffant et al., 2007). Hence, there is a great need for next-class kinase inhibitors that work through alternative mechanisms leading to higher target specificity.

A completely different approach can be used for the characterization of highly specific kinase inhibitors. The aim of this promising alternative avenue is to discover molecules that disrupt protein interactions involving protein kinases. We have recently developed and used a bioluminescence resonance energy transfer (BRET)-based screening assay (reviewed in Bacart et al., 2008) in yeast to discover first-in-class small-molecule inhibitors of the interaction between CDK5 and its activating subunit, p25 (Corbel et al., 2011). Here, we report the characterization of tamoxifen as new a CDK5/p25 interaction inhibitor from BRET-based screening of the Prestwick Chemical Library, a library composed of 100% marketed drugs with diverse clinical applications, thus representing a high degree of "drug-likeness". Our experiments show inhibition of the catalytic activity of CDK5 by binding of tamoxifen (TMX) on the neurotoxic activator, p25, opening up a new therapeutic perspective on the oldest and most-prescribed hormone therapy for breast cancer.

RESULTS

Tamoxifen (TMX) Inhibits Both CDK5/p25 and CDK5/p35 Protein-Protein Interactions

In order to characterize small chemical inhibitors of the interaction between CDK5 and its activating subunit, p25, we have used a BRET-based screening assay on the budding yeast *Saccharomyces cerevisiae*, which we developed previously (Corbel et al., 2011). In the presence of a substrate, bioluminescence from luciferase (*Renilla* luciferase, RLuc) excites the acceptor fluorophore (yellow fluorescent protein [YFP]) if the donor and acceptor are 10–100 Å apart, thus monitoring the molecular interaction between the fused proteins p25 and CDK5, respectively (Figure 1A). We previously showed that the BRET signal obtained is specific for the CDK5/p25 interaction; we estimated the signal/background (S/B) ratio to be ~10 (Corbel et al., 2011). The unspecific background of the BRET signal is mainly due to stochastic interactions between the donor and the acceptor inside the cells (Bacart et al., 2008). Hence, the BRET signal detected in yeast (~225 mBRET, Figure 1B) coexpressing CDK5-YFP and p25-RLuc fusion proteins appeared specific and robust enough to enable screening of chemical collections. Moreover, as already described (Corbel et al., 2011), we used inducible promoters such as the *GAL* promoter to enable the small molecules to first interact with one of the two partners prior to CDK5-YFP/p25-RLuc heterodimer formation. Screening small molecules against non-preformed protein complexes is likely to increase the hit rates (Hamdi and Colas, 2012). We screened the Prestwick Chemical Library composed of 100% approved drugs (US Food and Drug Administration, European Medicines Agency, and other agencies) for which bioavailability and toxicity studies have already been carried out in humans; therefore if bioactive hits have sufficient affinity for the target, they could be tested immediately in patients. The hit rate of the BRET-based screening was low (only one hit from the 880 molecules tested, corresponding to ~0.1%), indicative of the specificity and the stringency levels of the screening assay. Independently, TMX was also identified as a hit by the screening of a mechanistic diversity set (which consists of 879 compounds) provided by the National Cancer Institute (NCI). In comparison with the control treatment (DMSO), the BRET signal measured decreased by 28.6% (±13.9%, $p < 0.01$) in the presence of 40 μM TMX. The inactive compound (InaCpd), used here as a negative result, is 17β-estradiol, a chemical compound functionally close to TMX but structurally different. The p25 protein results from the proteolytic cleavage of p35. In order to monitor the interaction between CDK5 and p35, a similar BRET assay in yeast was used (described in Corbel et al., 2011). As shown in Figure 1B, TMX was also able to inhibit the CDK5/p35 interaction (–48.7% ± 5.98% [$p < 0.01$] of the BRET signal in the presence of 40 μM drug). As for the CDK5/p25 interaction, InaCpd has much less effect on CDK5/p35 than TMX (–9.4% ± 3.9% of control; $p < 0.05$).

In order to confirm the inhibition of the CDK5/p25 interaction by TMX, we next performed glutathione S-transferase (GST) pull-down assays on recombinant proteins, in the presence of increasing concentrations of the molecule. Similar to the BRET-based screening assay, TMX was first added on one monomer (here on 6xHis-p25) and not directly on the dimer. In line with the effect on BRET, TMX inhibited the interaction between GST-CDK5 and 6xHis-p25 in a dose-dependent way (Figure 1C). Quantification of the band intensities indicated that 7 μM TMX was able to inhibit half of the 6xHis-p25 binding to GST-CDK5 in this assay.

As neuroblastoma cell lines have already been shown to express p35 (Lee and Kim, 2004), they were chosen to validate the cellular effect of TMX. Expressions of p35, p25, CDK5, and tau were then checked in nine neuroblastoma cell lines (SH-SY5Y, SK-N-AS, SK-N-SH, SK-N-BE(2), LAN-1, LAN-5, BMMOA, IMR-32, and IGR-N-91). Among these, none expressed the cleaved protein p25 and only three simultaneously expressed a detectable amount of p35, CDK5, and one key protein substrate, the tau isoforms (Figure S1). The SK-N-BE(2) cell line was then selected by taking into account the expression

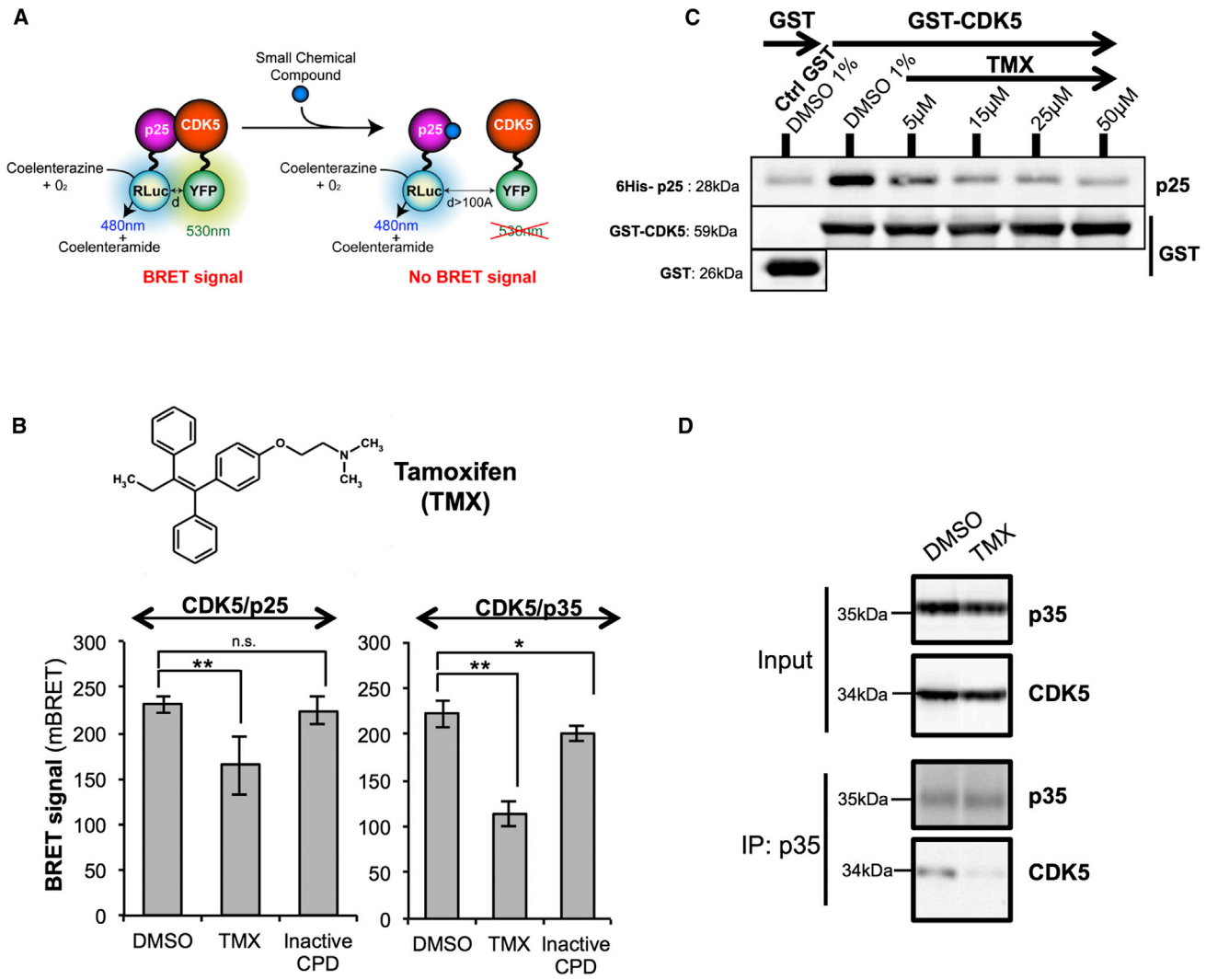

Figure 1. TMX Inhibits CDK5/p25 Interaction

(A) Schematic representation of the BRET-based screening assay (SCC, small chemical compound from a chemical library).

(B) BRET values obtained for yeast strains expressing CDK5-YFP and p25-RLuc or CDK5-YFP and p35-RLuc fusion proteins and treated with 1% DMSO, 40 μM TMX, or 40 μM inactive compound, InaCpd (mean ± SD, error bars represent SD, n = 3). Significance levels are $^{*}p < 0.05$; $^{**}p < 0.01$; n.s., not significant.

(C) Extracts of bacteria expressing 6xHis-p25 (28kDa) were incubated in the presence of increasing doses of TMX (5–50 μM TMX in 1% DMSO) or DMSO (1%) during 10 min at 4°C before adding GST-CDK5 (59 kDa) for 10 min at 4°C. The GST-CDK5/6xHis-p25 complexes were purified on glutathione affinity gel and analyzed by SDS-PAGE followed by western blotting using antibodies directed against p25 and GST. Recombinant GST (26 kDa) (first lane on the left side) is used here to characterize the unspecific binding of 6xHis-p25.

(D) Crude protein extracts of the SK-N-BE(2) cell line co-treated with DMSO (0.25%) or TMX (25 μM) and MG132 (30 μM) (an inhibitor of proteasome) were analyzed by SDS-PAGE followed by western blotting using antibodies directed against CDK5 and p35 (Inputs). These extracts were then immunopurified using anti-p35 antibody and analyzed by SDS-PAGE followed by western blotting using antibodies directed against p35 and CDK5 (IP: p35).

level of p35, CDK5, and tau. These cells were first treated with 25 μM TMX or 0.25% DMSO during 6 hr. To verify that these treatments did not modify the expression levels of CDK5 and p35, their amounts were evaluated for the two conditions. Although CDK5 expression was not modified, the level of p35 was lower in cells treated with TMX (Figure S1). Interestingly, it was previously described that the inhibition of CDK5 activity by (*R*)-roscovitine leads to stabilization of p35 (Sahlgren et al., 2003). The opposite effect observed here for TMX underlines that both drugs may have a different mode of interaction with CDK5/p25. We then tested MG132, a proteasome inhibitor, to block the putative degradation of p35 induced by TMX treatment. As shown in Figure 1D, treatment with MG132 stabilized the level of p35 in TMX-treated cells compared with the result obtained for DMSO. The cell extracts collected were then subjected to immunoprecipitation using p35 antibody and analyzed by SDS-PAGE followed by western blotting (Figure 1D). As expected, the level of CDK5 co-immunoprecipitated from the TMX-treated cell extracts was significantly reduced in comparison with the one obtained for DMSO treatment, confirming the modulation of CDK5/p25 interaction by TMX in the SK-N-BE(2) neuroblastoma cell line.

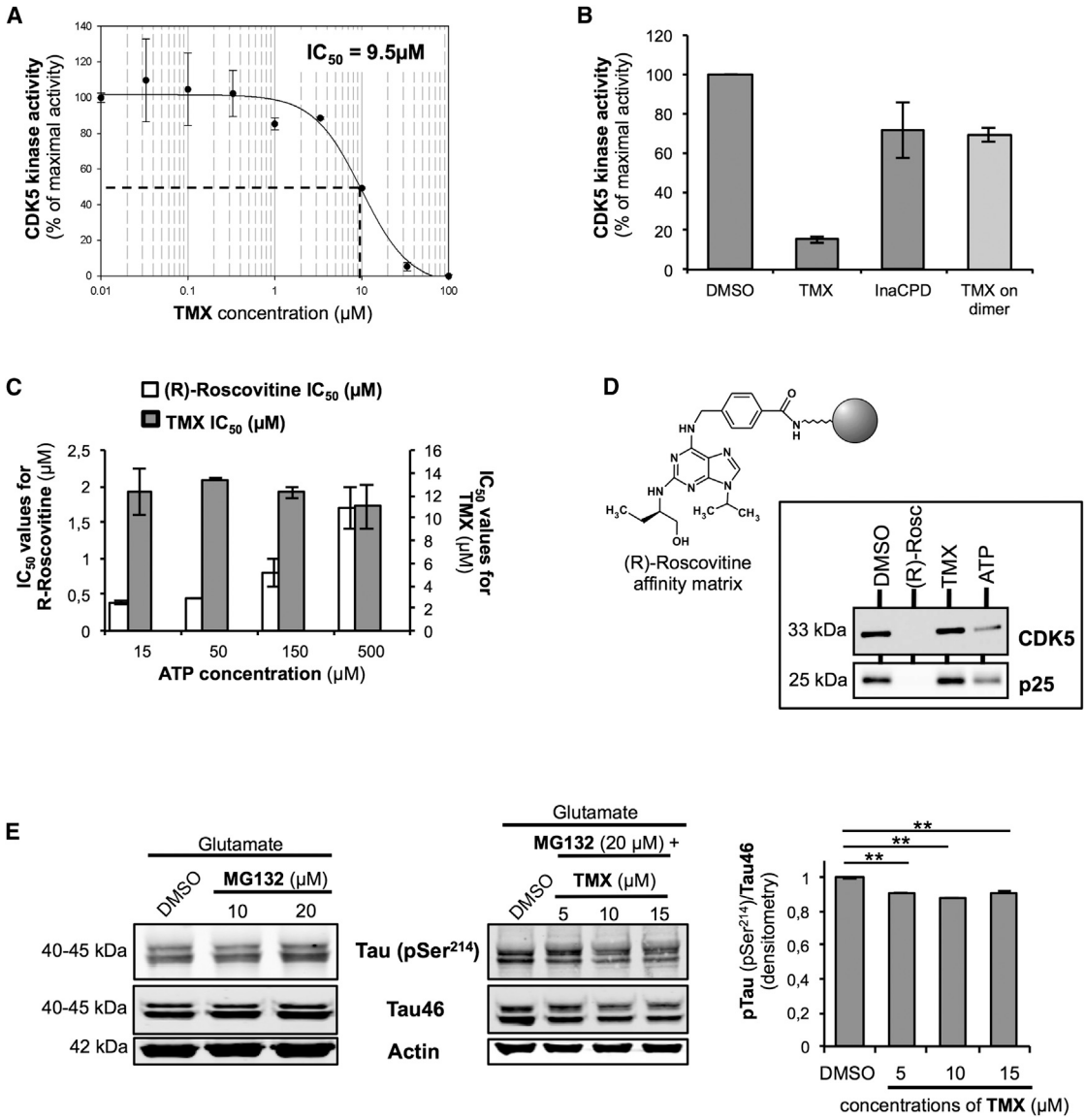

Figure 2. TMX Inhibits CDK5/p25 Activity In Vitro and in Primary Neuronal Cells

(A) Increasing doses of TMX were added to GST-CDK5 in the reaction mixture (incubation: 5 min on ice) before adding 6xHis-p25 (incubation: 25 min on ice). The kinase assay was then performed using histone H1 as substrate (incubation: 25 min at 30°C) (mean ± SD, error bars represent SD, n = 3).

(B) 33.3 μM TMX was added to the reaction mixture before the formation of the dimer or after the formation of the dimer (light gray histograms) (mean ± SD, error bars represent SD, n = 3). For comparison, the inactive compound was also added before the formation of the dimer (final concentration 33.3 μM).

(C) Increasing concentrations of ATP were added to the kinase reaction mixture and the resulting IC_{50} values were calculated for (*R*)-roscovitine and TMX (mean ± SD, error bars represent SD, n = 3).

(D) Analysis of the specificity of interaction between cellular components and the (*R*)-roscovitine affinity matrix by competition assay. Porcine brain extracts were supplemented with various concentrations of chemical compounds (500 μM for (*R*)-roscovitine, 2 mM for ATP, and 500 μM for TMX) before loading on to immobilized (*R*)-roscovitine. The bound proteins were analyzed by SDS-PAGE followed by western blotting using antibodies directed against CDK5 and p25.

(E) Left panel: treatment of primary neuronal cultures with 100 μM glutamate and increasing concentrations of MG132 over 5 hr has no consequence on the expression level of phospho-tau (pTau). Right panel: in the presence of 100 μM glutamate and 20 μM MG132, the addition of increasing concentrations of TMX decreases the phosphorylation of tau (pSer214). **Values are significantly decreased from DMSO. Mean ± SD, error bars represent SD, n (exposures) = 3.

TMX Inhibits Pathogenic CDK5/p25 Kinase Activity by Preventing the Formation of the Heterodimer

To validate the effect of TMX on the enzymatic activity of the target, we used an in vitro assay to examine the kinase activity of the CDK5/p25 recombinant complex. In order to mimic the BRET assay protocol used in yeast, we mixed TMX with CDK5 before adding p25. We next performed the protein kinase assay in the presence of increasing doses of TMX. In good agreement with the BRET experiments, we observed a dose-related inhibition of CDK5/p25 kinase activity by TMX, with a half maximal inhibitory concentration (IC_{50}) of 9.5 μM (Figure 2A). As previously observed for 3α-amino-5α-androstane (Corbel et al., 2011),

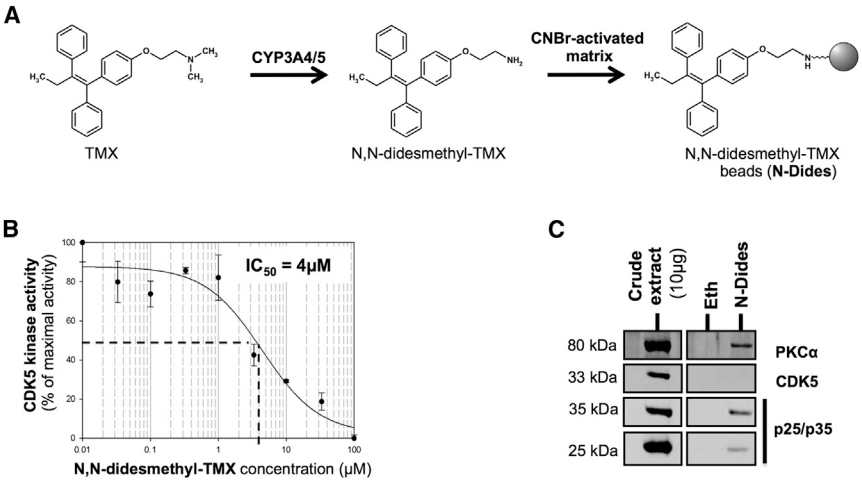

Figure 3. TMX Binds to p25 and Not to CDK5

(A) Schematic representation of the binding of N-Dides on CNBr-activated Sepharose through the primary amine group.

(B) Increasing doses of N-Dides were added to GST-CDK5 in the reaction mixture (incubation: 5 min on ice) before adding 6xHis-p25 (incubation: 25 min on ice). The kinase assay was then performed using histone H1 as substrate (incubation: 25 min at 30°C) (mean ± SD, error bars represent SD, n = 3).

(C) A porcine brain extract was loaded on control (ethanolamine [Eth]) and N-Dides matrices. Beads were extensively washed and the bound proteins were analyzed by SDS-PAGE followed by western blotting against CDK5, p35/p25, and PKCα.

another CDK5/p25 interaction inhibitor, TMX was less active when added on a CDK5/p25 preformed complex (–84.45% ± 1.82% of the kinase activity on monomers; –31.07% ± 3.71% on the preformed complex) (Figure 2B). In accordance with the BRET assay, kinase activity was less affected in the presence of InaCpd (–28.77% ± 14.4%).

To investigate the molecular mechanism of inhibition of the CDK5/p25 kinase by TMX, we next performed in vitro experiments with increasing doses of ATP in the kinase reaction mixtures. ATP modulation did not modify the IC_{50} of TMX significantly, indicating that the drug acts as a non-ATP competitor to inhibit kinase activity. As a control, with the same experimental conditions, ATP modification produced an effect on the level of kinase inhibition by (*R*)-roscovitine, a widely used ATP-mimetic inhibitor of CDK5 (Figure 2C).

To confirm this non-ATP mimic mechanism of inhibition, affinity chromatography was performed using (*R*)-roscovitine beads. Porcine brain extracts containing CDK5 and p25 were supplemented with various concentrations of DMSO, (*R*)-roscovitine, TMX, and ATP (Figure 2D). The signals corresponding to CDK5 and p25 disappeared in the presence of free (*R*)-roscovitine, decreased with the addition of ATP, but were unaffected by TMX. This confirms a different mode of binding of TMX to CDK5/p25 in comparison with (*R*)-roscovitine, a prototypic molecule for type I CDK inhibitors. To illustrate the non-conventional mode of kinase inhibition by TMX, the world's largest commercial kinase assay panel was assessed (KINOMEscan, DiscoveRx): 456 kinases belonging to the AGC, CAMK, CMGC, CK1, STE, TK, and TKL families and representing more than 80% of the human protein kinome were examined; 25 μM TMX was used. KINOMEscan assays report true thermodynamic interaction affinities, as opposed to IC_{50} values, which can depend on the ATP concentration. This active site-directed competition binding assay can detect multiple inhibitor types, including type I, type II, and allosteric. None of the kinases tested, including protein kinase C (PKC) isoforms (PRKCD, PRKCE, PRKCH, PRKCI, and PRKCQ) was strongly affected by TMX (Figure S2; Table S1).

For a more relevant model than neuroblastoma cell lines, validation of the effects of TMX on CDK5/p25 activity was then verified using primary neuronal cultures. CDK5 is a tau kinase and treatment with TMX should lead to a decrease in tau phosphorylation. Cells expressing the p25 subunit were preferred as the CDK5/p25 complex is more stable than CDK5/p35 (Patrick et al., 1999) and is thus more likely to have robust activity. As p25 was weakly expressed in primary cortical neuron cultures, cleavage of p35 was induced by glutamate, an excitatory amino acid involved in p25 production (Lee et al, 2000) (the appearance of p25 was verified by SDS-PAGE followed by western blotting; Figure S3). The proteasome inhibitor MG132 was used (Figure 2E) to avoid degradation of the protein p25 as previously observed after chemical treatments (Figure 1D). The addition of MG132 had no effect on the phosphorylation of tau (pSer214), a residue phosphorylated by CDK5 (Figure 2E, left panel) (Liu et al., 2002). In the presence of MG132 and increasing concentration of TMX, a decrease in tau phosphorylation was observed (Figure 2E, right panel). This decrease was significant in comparison with the variation observed for the signal of the anti-tau46 antibody, which recognizes all tau isoforms. This suggests that modification of the tau phosphorylation level probably results from a lower CDK5 kinase activity, itself caused by inhibition of the CDK5/p25 interaction by TMX.

TMX Binds to p25 and Not to CDK5

With the aim of detecting TMX targets, affinity chromatography was used. We took advantage of a product of TMX metabolism, *N,N*-didesmethyl-TMX (N-Dides) (Figure 3A), as already described (O'Brian et al., 1988a). N-Dides was coupled to CNBr-activated Sepharose through its primary amine. In order to check that N-Dides was still active, its effect on CDK5/p25 kinase activity was measured (Figure 3B). Kinase activity of CDK5 was also affected by N-Dides (IC_{50} = 4 μM) (Figure 3B). Hence, affinity chromatography using this immobilized metabolite was suitable for studying TMX selectivity. Porcine brain extract was used as the protein source, as it contains desired targets of TMX: CDK5, p35, p25, and PKCα (protein kinase C α) (Figure 3C, left panel). PKCα was used as control as its binding to TMX has already been described (O'Brian et al., 1988a). The signal obtained using anti-PKCα antibody indicated that the N-Dides matrix was functional. In addition, western blot analysis revealed the presence of p35 and p25 on the beads, whereas CDK5 was absent (Figure 3C, right panel). This experiment revealed that TMX can bind to the p35 or p25 activators, rather than to the CDK5 monomer.

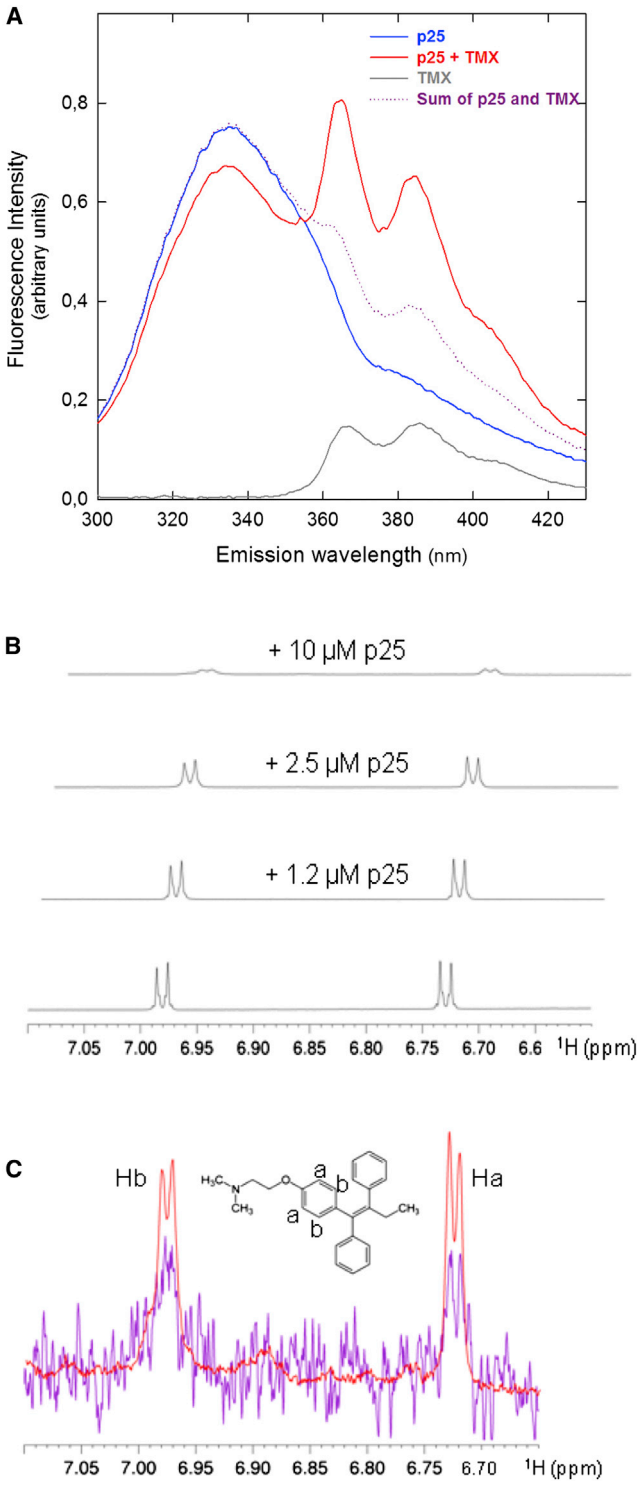

Figure 4. Biophysical Characterizations of the p25-TMX Complex

(A) Fluorescence emission spectra of free p25 (blue) and TMX-bound p25 forms (red) in 50 mM Tris-HCl (pH 7.5), 140 mM KCl, 0.1 mM EDTA, 1 mM DTT, 10% glycerol, 20°C. Fluorescence emission spectrum of free TMX is shown in gray. The arithmetic sum of the free forms of p25 and TMX is also displayed (purple) for comparison with the complex experimental spectrum. Excitation wavelength is 290 nm, protein concentration 1 µM, TMX 1.5 µM.

(B) 1D NOESY spectra of TMX showing signals of the aromatic moieties from bottom to top: 100 µM TMX without p25, and with 1.2 µM, 2.5 µM, and 10 µM p25.

(C) Superposition of the same aromatic region of the 1D NOESY ^{1}H spectrum of TMX (in red) and the saturation difference in the presence of 10 µM p25, overlaid in purple.

Binding Mode of TMX on the p25 Protein Surface

The protein p25 contains three tryptophanyl residues among its 208 residues: W177, W190, and W258 (numbering of residues referring to the entire p35 protein chain). Figure 4A displays the tryptophan fluorescence emission spectrum of p25 in the absence and in the presence of TMX. Upon addition of TMX to a p25 solution, a decrease in the tryptophan emission spectrum was observed. This result confirmed that TMX interacts with p25 with subsequent conformational changes within the protein. Whatever the protein binding status, free or complexed, the maximal emission wavelength of the fluorescent tryptophan residues remains at 335nm; it can be inferred that the conformational modifications induced by the binding to TMX do not affect protein polarity in the surroundings of these aromatic residues. In addition, TMX excited at 290 nm exhibited two emission bands at 366 and 386 nm. The intensity of these bands was increased upon TMX binding to p25. This enhancement might result from a non-radiative energy transfer from tryptophan to TMX, which implies that these two fluorophores are close to each other and/or that modification of the emission transition dipole moments of TMX occurs. In the latter case, the decrease in emission of the tryptophans could be due to the presence of side chains in the vicinity of one or some tryptophanyl residues, which would quench the Trp emissions within the p25-TMX complex.

Interaction of p25 with TMX was further confirmed by TMX nuclear magnetic resonance (NMR) spectroscopy in the absence or presence of p25. In a first series of experiments, titration of the p25 protein into the TMX solution resulted in chemical shift perturbations and broadening of several peaks of the chemical compound in a dose-dependent manner (Figure 4B). Perturbations of the signal could be observed in the region of aromatic proton resonances in the TMX spectrum, indicative of binding of the protein to these moieties (Figures 4B and 4C; Figure S4). The aliphatic region showed additional perturbations of the signals, indicating that most of the molecule is implicated in the interaction. In addition, saturation transfer experiments were performed with the sample containing TMX mixed with p25 in a 10:1 ratio. The protein was saturated by an impulsion at −1 ppm, a frequency outside the TMX range. This saturation will thus be transferred to the small molecule by spin diffusion only if it is bound by the protein. In addition, an off-resonance spectrum of TMX was acquired as a control spectrum with saturation at 300 ppm, outside the resonance range of both TMX and p25. Detection of several signals in the red difference spectrum (Figure 4C) between the on and off-saturation experiments confirmed the interaction. Signals corresponding to aromatic protons and aliphatic protons (Figure S4) could be identified in the difference spectrum, indicating the involvement of these chemical moieties in the binding.

In silico analysis revealed that TMX can dock to an active site on p25, where the amino acids of the C-helix of CDK5 (Figure 5A) are accommodated. This in silico docking is congruent with the

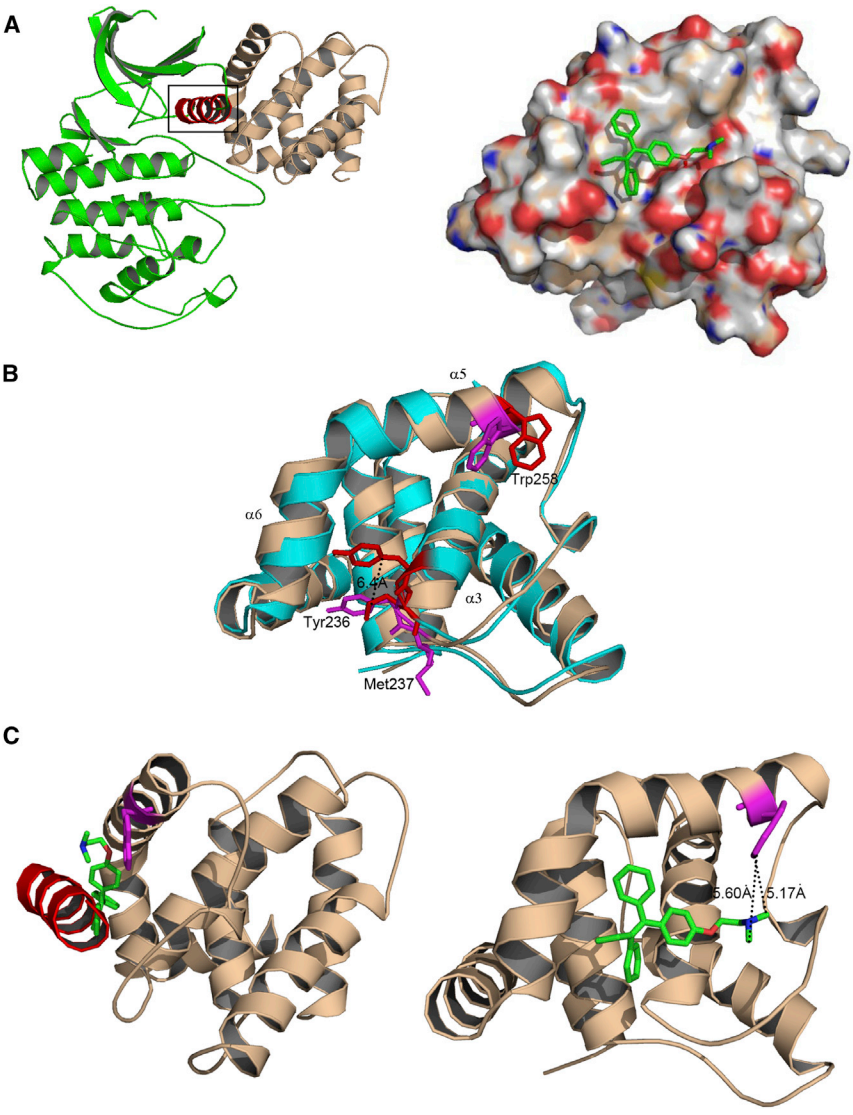

Figure 5. In Silico Analysis of the TMX Binding on p25

(A) Left panel: two hot spots are described between p25 and CDK5. The hot spot studied here concerns the αC helix of CDK5 (in red) (which contains the conserved motif of CDKs: PSAALRE) and p25. Right panel: the positively/negatively charged sections of the p25 surface are depicted in red and blue, respectively. A cavity, which can host TMX, is observed on the p25 surface.

(B) The conformational changes and deviations of the α helix. The original conformation of p25 is colored in cyan and the structure from the molecular dynamics simulations is wheat colored. Amino acids from the original p25 are in red and those from the simulations are in purple. The structures of TMX are omitted for clarity.

(C) Representations of the binding patterns of TMX on the protein p25 obtained after dynamic simulations. TMX is represented in green and the Trp in position 258 is purple. The right panel shows the proximity between TMX and the protein, and more particularly with Trp258 (5.17 and 5.60 Å).

affinity chromatography experiment (Figure 3). The portion of the drug linked to Sepharose extends toward the solvent, compatible with the binding of TMX targets. According to our simulations, most of the protein stayed stable during the dynamics processes; compared with the original p25 structure, only certain deviations or conformational changes were observed in the α helix around the active site in the simulated protein. For example, as seen in Figure 5B, the deviation of α5 and α6 is obvious. Due to the conformational changes in the tail of α3, Tyr236 deviated from the original position by a distance of 6.4 Å. All these deviations or conformational changes were caused by the binding of TMX to p25. The conformational change of Trp258 is shown in Figure 5C; the distance between the side chain of the residue in the new position and TMX is less than 6 Å.

DISCUSSION

Here we report that TMX (Jordan, 2003), the gold standard for endocrine treatment of all stages of estrogen-receptor-positive breast cancer, inhibits CDK5 kinase activity by blocking the binding of CDK5 to its regulatory subunit p35 or its N-terminal truncated form p25. The inhibition of CDK5 is crucial as this kinase is involved in numerous pathological processes (neurodegenerative diseases such as tauopathies, pancreatic and prostatic cancers, lung cancer). Although TMX is successfully used in the clinic for the treatment of cancer, it was initially identified in the early 1960s as a contraceptive agent (Harper and Walpole, 1967). The first targeted medicine for breast cancer is in fact the result of a therapeutic repositioning. The chemical library screened in this study was designed to enable drug repositioning.

Our present findings add CDK5/p35 and CDK5/p25 to the selectivity pattern of TMX (Figure 6) and could be useful to interpret its cellular actions in a more detailed manner. TMX is a triphenylethylenic selective estrogen receptor modulator; it acts mainly via estrogen receptors (ER). TMX is cytostatic on ER-positive cell lines at low concentrations closed to its binding affinity ($K_d \approx 1$ nM) for ER. At higher concentrations (1–10 μM), the cytotoxic effect of TMX is not reversed by the natural ligand of ER, 17β-estradiol (E2), suggesting other targets (de Medina et al., 2004). Studies on the pharmacological selectivity of TMX have indicated that this cellular effect can be explained through nanomolar to micromolar affinity binding to various other cellular components (Figure 6).

The kinase activity of CDK5 is not only linked to neurodegenerative disease but also to cancer. Studies have shown that CDK5 promotes glioblastoma cell migration and invasion by phosphorylation of phosphatidylinositol 3-kinase enhancer-A

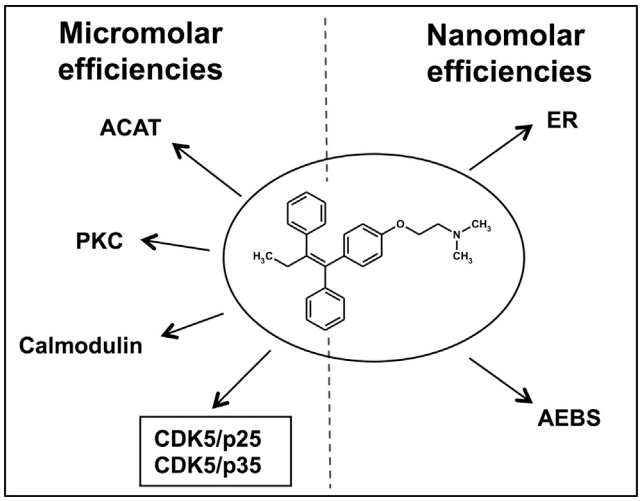

Figure 6. TMX and Its Main Targets

Acyl-coenzyme A:cholesterol acyltransferase (ACAT); protein kinase C (PKC); calmodulin (CaM)-dependent enzymes (Calmodulin); estrogen receptor (ER); microsomal anti-estrogen binding site (AEBS). Adapted from de Medina et al. (2004).

GTPase. This increased glioblastoma cell migration can be significantly attenuated by roscovitine (Liu et al., 2008), a chemical compound also used in the present study as an ATP-mimetic inhibitor of CDK5 (Figure 2). Interestingly, TMX can significantly inhibit human glioblastoma cell invasion in vitro. This effect is linked to the inhibition of protein kinase C (PKC) activity as described by the authors (Zhang et al., 1997). The inhibition of PKC was the mechanism suspected to mediate the cellular effect of TMX on cancer cell migration. This mechanism was used for phase 2 clinical trials conducted with TMX for glioma treatment (Rich and Bigner, 2004). The level of PKC inhibition by TMX varies from 25 μM to 100 μM (O'Brian et al., 1985, 1986). TMX inhibits PKC by binding to the ATP-binding region of the active site as observed by affinity chromatography (O'Brian et al., 1988b). In our present study, we obtained an N-Dides matrix in order to purify both PKCα and the p25 activating subunit from porcine brain (Figure 3). Our results suggest that the inhibition of CDK5/p25 could contribute to the antitumor effect of TMX. Additional studies will be needed to fully understand the contribution of this inhibition to the overall effect of the drug on glioblastoma cells.

The BRET-based screening assay used in our study is well adapted for the discovery of protein-protein interaction inhibitors. One of the main challenges in pharmacology is to characterize selective inhibitors that bind with high affinity to a specific target without significantly affecting similar protein targets. By binding to the protein surface distant from the ATP-binding site, TMX targets a less conserved region. Our previous work (Corbel et al., 2011; Zhang et al., 2011) has shown that destabilization of the dimer with small chemical drugs (3α-amino-5α-androstane) seems to be very hard to observe, because all the characterized compounds are inactive on the CDK5/p25 preformed dimer. The inability of TMX to disrupt preformed CDK5/p25 complexes (Figure 2B) highlights the principle that screening small molecules against non-preformed protein complexes is likely to increase hit rates.

Another non-ATP competitive-based strategy has been developed previously to inhibit CDK5 selectively (Sundaram et al., 2013) by a peptide (CIP) derived from p35. CIP specifically inhibits hyperactivation of CDK5 both in vitro and in cellular assays. Interestingly, the sequence of this peptide contains residues 157–279 of p35, including the Trp258 putatively involved in the interaction with TMX as revealed by our in silico and fluorescence experiments (Figure 5B). The inhibition by CIP showed that it is possible to specifically modulate CDK5/p25 kinase activity without significantly affecting the CDK5/p35 dimer (Sundaram et al., 2013). Nevertheless, and despite the specificity for the pathogenic dimer CDK5/p25, CIP is clearly not adapted for human therapy compared with small chemical molecules. However, its high specificity clearly demonstrates the potential of using a non-ATP competitor as inhibitor of CDK5/p25. Although TMX is a marketed drug, medicinal chemistry and structure-activity relationship (SAR) studies would be beneficial to characterize TMX derivatives that can specifically block the CDK5/p25 interaction with higher efficiency. The neuroprotective effect of TMX has already been described (O'Neill et al., 2004) and attributed to the partial estrogen agonist role of TMX in the brain. The data described in this article suggest that a CDK5-dependent mechanism may contribute to this effect.

To ensure that the reduction of CDK5/p25 dimer formation resulted in decreased phosphorylated forms of tau, we performed western blot analysis using phospho-tau antibodies directed against pSer214. Despite the fact that Ser214 is not followed by a proline residue, this site seems to be affected by inhibition of CDK5 by TMX. Phosphorylation of non-(Ser/Thr) Pro sequences by CDK5 are reported in the literature: Ser20 (PLSQETFsDLWKLLP) (Ajay et al., 2010) and Ser15 (PSVEPPLsQETFSDL) (Lee et al., 2007) of p53; Thr197 (ILTPKKHtVKKRIGS) of Rho family GTP-binding protein TC10alpha (Okada et al., 2008). Moreover, the phosphorylation of tau on Ser214 by CDK5 has also been reported (Liu et al., 2002). These data indicate that Ser214 should be considered as a bona fide marker of CDK5 kinase activity.

Surprisingly, a recent study indicates that the p25 subunit preferentially binds and activates glycogen synthase kinase 3β (GSK3β) (Chow et al., 2014). GSK3β phosphorylates tau and its 3D structure is remarkably similar to CDK5. The four residues of p25 predicted to establish hydrogen bonds with GSK3β (Trp190, Gly238, Met237, and Asp259) surround the predicted site that accommodates TMX, as depicted in Figure S5. One of our aims now is to analyze biochemically the effect of TMX on the GSK3β/p25 interaction. In the context of discovery of small molecular size protein-protein interaction inhibitors, our study sheds light on a very important hot spot on the p25 surface. This region of p25 can be considered as a starting point for further development of new potent and selective pharmacological inhibitors. Our study provides a good illustration of the relevance of protein-protein interactions as therapeutic targets of great potential.

A therapeutic link between TMX and AD was already underlined in an epidemiologic study (Breuer and Anderson, 2000). Observations on 93,031 women (at least 65 years old) revealed that women receiving TMX were less likely to be diagnosed with Alzheimer's disease. It is estimated that more than

400,000 women are alive today as a result of TMX therapy. Our study suggests that this fascinating molecule might bring new benefits to human kind in the future by inspiring new treatments against neurodegenerative diseases.

SIGNIFICANCE

CDK5 activity is misregulated following its interaction with the pathological subunit p25. Most drug-like inhibitors of CDK5/p25 already described target the ATP-binding pocket and consequently are mostly poorly selective. Inhibition of side targets could lead to side effects that are non-compatible with treatment of human neuropathies such as Alzheimer's disease (AD). To address this problem, a BRET-based screening assay has been developed with the aim of characterizing inhibitors of the CDK5/p25 interaction.

Among the compounds screened, TMX, a generic drug used for breast cancer treatment, was characterized as a hit molecule. We showed here that TMX acts by binding on the protein p25 subunit and that TMX treatment of neuronal cells modulates the pattern of tau phosphorylation, a known substrate of CDK5/p25 and one of the neuropathological hallmarks of AD. This study reveals that TMX binds to a druggable hot spot on the p25 surface. This hot spot can be used to develop new therapeutic strategies for CDK5/p25-related diseases.

EXPERIMENTAL PROCEDURES

Chemicals

MG132 (no. C2211), glutamate (no. G1251), TMX (no. T5648), and 17β-estradiol (no. E8875) were purchased from Sigma. DMSO (no. 472301, Sigma) is the drug vehicle used in this study.

BRET Assay in Yeast

BRET signals were measured as described previously in Corbel et al. (2011) (see Supplemental Information for details).

Neuroblastoma Cell Line Culture

The SK-N-BE(2) human neuroblastoma cell line was kindly provided by Dr. J. Bernard (UMR8126, Institut Gustave Roussy, Villejuif, France). Cells at 60% confluence were treated with 30 μM MG132 and 25 μM chemical compounds for 6 hr before lysis. Crude protein extracts were prepared in RIPA buffer (Supplemental Information) and analyzed by SDS-PAGE followed by western blotting or after immunoprecipitation using anti-p35 antibody.

Protein Kinase Assays

The recombinant mammalian proteins CDK5 and p25 are expressed in *Escherichia coli* as a GST-fusion (GST-CDK5) or a His-tagged protein (6xHis-p25). These two proteins were purified using glutathione agarose (no. G4510, Sigma) and Ni-NTA agarose (no. 30210, Qiagen) matrices following the manufacturers' recommendations. To perform the kinase activity measurements, the two proteins were mixed separately (dimer in formation) or together (dimer formed) before adding the compound studied. Then, the kinase activities were assayed using histone H1 as substrate in buffer C (Supplemental Information) for 25 min at 30°C, at a final ATP concentration of 15 μM. For the ATP competition assays, the final concentration of ATP was modified. To measure the IC_{50}, the curve fitting software SigmaPlot and the Miller curve fitting algorithm were used. These experiments were performed on the Kinase Inhibitor Specialized Screening facility (KISS*f*), a member of Biogenouest (Western France Life Science and Environment Core Facility Network).

Affinity Chromatography on Immobilized Matrices

(*R*)-Roscovitine and N-Dides affinity matrices were used according to the protocol previously described in Bach et al. (2005) (see Supplemental Information for details).

Electrophoresis and Western Blotting

Details on the classical protocols used are provided in the Supplemental Information. The primary antibodies used were p35/p25 (no. sc-820; Santa Cruz Biotechnology), CDK5 (no. sc-173; Santa Cruz Biotechnology), GST (no. sc-138; Santa Cruz Biotechnology), PKCα (no. 2056; Cell Signaling), tau (T46: no. 13-6400, Invitrogen), phospho-tau (pSer214: no. 54967, Anaspec), and β-actin (no. A5441, Sigma).

Ethics Approval

All animal care procedures were reviewed by the Institutional Animal Care Committee at the University of California, Santa Barbara, and found to be in compliance with guidelines on animal care.

Primary Cortical Neuronal Cultures

E18 pregnant Sprague-Dawley rats were purchased from Charles River Laboratories. Embryos were surgically removed and their cortices were dissected and cultured as described in Nikolic et al. (1996). Cortical cultures were grown in basal growth medium on six-well plates coated with poly-D-lysine; 400,000 cells were plated per well. Treatments with glutamate, MG132, and chemical compounds were performed 10 days after plating for 5 hr. The corresponding protocol is described in Lee et al. (2000). The cells were then retrieved, lysed in RIPA buffer, and the corresponding proteins were analyzed by western blotting.

Emission Spectrum of Tryptophanyl Residues of Free and TMX-Bound p25 Protein

Experiments were carried out with 1 μM purified 6xHis-p25 and 1.5 μM TMX prepared in buffer A (Supplemental Information). The protein concentration was determined by absorbancy measurements at 280 nm, using a molar extinction coefficient of 26,930 M^{-1} cm^{-1}. Trp fluorescence emission spectra were collected with an SLM 8100 spectrofluorometer at an excitation wavelength of 290 nm and 20°C. The optical path lengths were 0.4 cm for the excitation and 1 cm for the emission. The bandwidths of the excitation and the emission slits were 2 nm. The emission spectra were collected with 1 nm wavelength increments and the fluorescence intensities were corrected for the buffer contribution.

NMR

1D proton spectra were recorded on a 900-MHz spectrometer equipped with a cryoprobe head. TMX was first suspended in DMSO-d_6 before dilution into the NMR buffer (Supplemental Information). Selective saturation of protein resonances was done at –1 ppm or –900 Hz (saturation on spectrum) to excite the protein but not TMX. A control experiment was performed with TMX alone to ensure that the –1 ppm saturation pulse did not reach the compound. Off-saturation pulses were performed at 300 ppm. Spectra were acquired with 512 scans. Data processing and analysis was performed using Topspin 2.1. The proton TMX signal assignment is published in Cai et al. (2010).

Docking and Molecular Dynamics Simulations

The structure of p25 was obtained from the CDK5/p25 complex (PDB code: 1UNL) and the docking of TMX to the protein, energy filtering, and ranking were performed using the Glide module in the Schrodinger software suite (Friesner et al., 2004). The CA atom of Leu49 of CDK5 was adopted as the center of the enclosing docking box to confine TMX. The molecular dynamics simulations were carried out using the Amber 9.0 (Case et al., 2006) software suite with the all-atom force field of Cornell et al. (1995). A 2-fs time step was used and long-range electrostatic interactions were treated with the particle mesh Ewald procedure (Darden et al., 1993) using a cubic B-spline interpolation and a 10^{-5} tolerance for the direct space, and with a 12-Å non-bonded cutoff. Minimization consisted of four steps and all the heavy atoms in the p25/TMX complex were restrained with degressive forces of 500, 100, and 5 kcal/mol, respectively. The production parts of all the systems took 10 ns in the NPT ensemble at 300 K with Berendsen temperature coupling and at constant

pressure (1 atm) with isotropic molecule-based scaling (Berendsen et al., 1984).

Statistical Analysis

Data were expressed as means ± SD. Statistical analyses were done by Student's *t* test and significance levels are $^{*}p < 0.05$; $^{**}p < 0.01$; n.s., not significant.

SUPPLEMENTAL INFORMATION

Supplemental Information includes Supplemental Experimental Procedures, five figures, and one table and can be found with this article online at http://dx.doi.org/10.1016/j.chembiol.2015.03.009.

AUTHOR CONTRIBUTIONS

Ca.C., B.Z., P.C., C.C., K.S.K., I.L., V.L.T., and S.B. designed the research; Ca.C., B.Z., A.L.P., I.L., B.B., V.L.T., and S.B. performed research; Ca.C., B.Z., I.L., P.C., C.C., K.S.K., V.L.T., and S.B. analyzed the data, Ca.C., B.Z., I.L.,V.L.T., and S.B. wrote the paper.

ACKNOWLEDGMENTS

Dr. S. Ruchaud is warmly acknowledged for her continuing support. We would like to thank Dr. G. Gamboa da Costa and Pr. M. Marques for providing *Z*-*N*,*N*-didesmethyltamoxifen; Dr. L. Meijer for providing (*R*)-roscovitine Sepharose matrices; N. Desban, Dr. A. Hamdi, and C. Delehouzé for cell culture; Y. Ferandin for kinase assays; S. Chatterjee and K. Günther for preparing primary neuronal cultures; Dr. B. Fritzinger for data acquisition on the spectrometer; Biogenouest and Cancéropôle Grand-Ouest (axis: Natural Sea Products in Cancer Treatment) for continuing support. The NMR facilities were funded by the Région Nord, CNRS, Pasteur Institute of Lille, European Community (FEDER), French Research Ministry, and the University of Sciences and Technologies of Lille I. We acknowledge support from the TGE RMN THC (FR-3050, France). Ca.C. is supported by the Région Bretagne (ARED no. 3358), CNRS, and the Association pour la Recherche contre le Cancer (ARC); P.C. is supported by a CNRS PIR grant; S.B. is supported by ARC (contract ARC3889), ANR/Investissements d'Avenir program by means of the OCEANOMICs project (grant no. ANR-11-BTBR-0008) and INCa (NECROTRAIL Program).

Received: December 15, 2014
Revised: February 27, 2015
Accepted: March 6, 2015
Published: April 9, 2015

REFERENCES

Ajay, A.K., Upadhyay, A.K., Singh, S., Vijayakumar, M.V., Kumari, R., Pandey, V., Boppana, R., and Bhat, M.K. (2010). Cdk5 phosphorylates non-genotoxically overexpressed p53 following inhibition of PP2A to induce cell cycle arrest/apoptosis and inhibits tumor progression. Mol. Cancer *9*, 204.

Bacart, J., Corbel, C., Jockers, R., Bach, S., and Couturier, C. (2008). The BRET technology and its application to screening assays. Biotechnol. J. *3*, 311–324.

Bach, S., Knockaert, M., Reinhardt, J., Lozach, O., Schmitt, S., Baratte, B., Koken, M., Coburn, S.P., Tang, L., Jiang, T., et al. (2005). Roscovitine targets, protein kinases and pyridoxal kinase. J. Biol. Chem. *280*, 31208–31219.

Berendsen, H.J.C., Postma, J.P.M., van Gunsteren, W.F., Di-Nola, A., and Haak, J.R. (1984). Molecular dynamics with coupling to an external bath. J. Chem. Phys. *81*, 3684–3690.

Bharate, S.B., Sawant, S.D., Singh, P.P., and Vishwakarma, R.A. (2013). Kinase inhibitors of marine origin. Chem. Rev. *113*, 6761–6815.

Breuer, B., and Anderson, R. (2000). The relationship of tamoxifen with dementia, depression, and dependence in activities of daily living in elderly nursing home residents. Women Health *31*, 71–85.

Cai, C., Chen, X., and Ge, F. (2010). Analysis of interaction between tamoxifen and ctDNA in vitro by multi-spectroscopic methods. Spectrochim. Acta A Mol. Biomol. Spectrosc. *76*, 202–206.

Case, D.A., Darden, T.A., Cheatham, T.E., III, and Simmerling, C.L. (2006). AMBER 9. (University of California San Francisco).

Chow, H.M., Guo, D., Zhou, J.C., Zhang, G.Y., Li, H.F., Herrup, K., and Zhang, J. (2014). CDK5 activator protein p25 preferentially binds and activates GSK3beta. Proc. Natl. Acad. Sci. USA *111*, E4887–E4895.

Cohen, R.M., Rezai-Zadeh, K., Weitz, T.M., Rentsendorj, A., Gate, D., Spivak, I., Bholat, Y., Vasilevko, V., Glabe, C.G., Breunig, J.J., et al. (2013). A transgenic Alzheimer rat with plaques, tau pathology, behavioral impairment, oligomeric abeta, and frank neuronal loss. J. Neurosci. *33*, 6245–6256.

Contreras-Vallejos, E., Utreras, E., and Gonzalez-Billault, C. (2012). Going out of the brain: non-nervous system physiological and pathological functions of Cdk5. Cell. Signal. *24*, 44–52.

Corbel, C., Wang, Q., Bousserouel, H., Hamdi, A., Zhang, B., Lozach, O., Ferandin, Y., Tan, V.B., Gueritte, F., Colas, P., et al. (2011). First BRET-based screening assay performed in budding yeast leads to the discovery of CDK5/p25 interaction inhibitors. Biotechnol. J. *6*, 860–870.

Cornell, W.D., Cieplak, P., Bayly, C.I., Gould, I.R., Merz, K.M., Ferguson, D.M., Spellmeyer, D.C., Fox, T., Caldwell, J.W., and Kollman, P.A. (1995). A second generation force field for the simulation of proteins,nucleic acids, and organic molecules. J. Am. Chem. Soc. *117*, 5179–5197.

Cruz, J.C., and Tsai, L.H. (2004). Cdk5 deregulation in the pathogenesis of Alzheimer's disease. Trends Mol. Med. *10*, 452–458.

Darden, T., York, D., and Pedersen, L. (1993). Particle mesh Ewald: an N.log(N) method for Ewald sums in large systems. J. Chem. Phys. *98*, 10089–10092.

de Medina, P., Favre, G., and Poirot, M. (2004). Multiple targeting by the antitumor drug tamoxifen: a structure-activity study. Curr. Med. Chem. Anticancer Agents *4*, 491–508.

Dhavan, R., and Tsai, L.H. (2001). A decade of CDK5. Nat. Rev. Mol. Cell Biol. *2*, 749–759.

Feldman, H.H., Haas, M., Gandy, S., Schoepp, D.D., Cross, A.J., Mayeux, R., Sperling, R.A., Fillit, H., van de Hoef, D.L., Dougal, S., et al. (2014). Alzheimer's disease research and development: a call for a new research roadmap. Ann. N Y Acad. Sci. *1313*, 1–16.

Feldmann, G., Mishra, A., Hong, S.M., Bisht, S., Strock, C.J., Ball, D.W., Goggins, M., Maitra, A., and Nelkin, B.D. (2010). Inhibiting the cyclin-dependent kinase CDK5 blocks pancreatic cancer formation and progression through the suppression of Ras-Ral signaling. Cancer Res. *70*, 4460–4469.

Friesner, R.A., Banks, J.L., Murphy, R.B., Halgren, T.A., Klicic, J.J., Mainz, D.T., Repasky, M.P., Knoll, E.H., Shelley, M., Perry, J.K., et al. (2004). Glide: a new approach for rapid, accurate docking and scoring. 1. Method and assessment of docking accuracy. J. Med. Chem. *47*, 1739–1749.

Goodyear, S., and Sharma, M.C. (2007). Roscovitine regulates invasive breast cancer cell (MDA-MB231) proliferation and survival through cell cycle regulatory protein cdk5. Exp. Mol. Pathol. *82*, 25–32.

Guiffant, D., Tribouillard, D., Gug, F., Galons, H., Meijer, L., Blondel, M., and Bach, S. (2007). Identification of intracellular targets of small molecular weight chemical compounds using affinity chromatography. Biotechnol. J. *2*, 68–75.

Hamdi, A., and Colas, P. (2012). Yeast two-hybrid methods and their applications in drug discovery. Trends Pharmacol. Sci. *33*, 109–118.

Harper, M.J., and Walpole, A.L. (1967). A new derivative of triphenylethylene: effect on implantation and mode of action in rats. J. Reprod. Fertil. Suppl. *13*, 101–119.

Jordan, V.C. (2003). Tamoxifen: a most unlikely pioneering medicine. Nat. Rev. Drug Discov. *2*, 205–213.

Laha, J.K., Zhang, X., Qiao, L., Liu, M., Chatterjee, S., Robinson, S., Kosik, K.S., and Cuny, G.D. (2011). Structure-activity relationship study of 2,4-diaminothiazoles as Cdk5/p25 kinase inhibitors. Bioorg. Med. Chem. Lett. *21*, 2098–2101.

Lee, J.H., and Kim, K.T. (2004). Induction of cyclin-dependent kinase 5 and its activator p35 through the extracellular-signal-regulated kinase and protein

kinase A pathways during retinoic-acid mediated neuronal differentiation in human neuroblastoma SK-N-BE(2)C cells. J. Neurochem. *91*, 634–647.

Lee, M.S., Kwon, Y.T., Li, M., Peng, J., Friedlander, R.M., and Tsai, L.H. (2000). Neurotoxicity induces cleavage of p35 to p25 by calpain. Nature *405*, 360–364.

Lee, J.H., Kim, H.S., Lee, S.J., and Kim, K.T. (2007). Stabilization and activation of p53 induced by Cdk5 contributes to neuronal cell death. J. Cell. Sci. *120*, 2259–2271.

Lew, J., Winkfein, R.J., Paudel, H.K., and Wang, J.H. (1992). Brain proline-directed protein kinase is a neurofilament kinase which displays high sequence homology to p34cdc2. J. Biol. Chem. *267*, 25922–25926.

Liu, F., Iqbal, K., Grundke-Iqbal, I., and Gong, C.X. (2002). Involvement of aberrant glycosylation in phosphorylation of tau by cdk5 and GSK-3beta. FEBS Lett. *530*, 209–214.

Liu, R., Tian, B., Gearing, M., Hunter, S., Ye, K., and Mao, Z. (2008). Cdk5-mediated regulation of the PIKE-A-Akt pathway and glioblastoma cell invasion. Proc. Natl. Acad. Sci. USA *105*, 7570–7575.

Malumbres, M., and Barbacid, M. (2005). Mammalian cyclin-dependent kinases. Trends Biochem. Sci. *30*, 630–641.

Meijer, L., Borgne, A., Mulner, O., Chong, J.P., Blow, J.J., Inagaki, N., Inagaki, M., Delcros, J.G., and Moulinoux, J.P. (1997). Biochemical and cellular effects of roscovitine, a potent and selective inhibitor of the cyclin-dependent kinases cdc2, cdk2 and cdk5. Eur. J. Biochem. *243*, 527–536.

Mettey, Y., Gompel, M., Thomas, V., Garnier, M., Leost, M., Ceballos-Picot, I., Noble, M., Endicott, J., Vierfond, J.M., and Meijer, L. (2003). Aloisines, a new family of CDK/GSK-3 inhibitors. SAR study, crystal structure in complex with CDK2, enzyme selectivity, and cellular effects. J. Med. Chem. *46*, 222–236.

Nikolic, M., Dudek, H., Kwon, Y.T., Ramos, Y.F., and Tsai, L.H. (1996). The cdk5/p35 kinase is essential for neurite outgrowth during neuronal differentiation. Genes Dev. *10*, 816–825.

O'Brian, C.A., Liskamp, R.M., Solomon, D.H., and Weinstein, I.B. (1985). Inhibition of protein kinase C by tamoxifen. Cancer Res. *45*, 2462–2465.

O'Brian, C.A., Liskamp, R.M., Solomon, D.H., and Weinstein, I.B. (1986). Triphenylethylenes: a new class of protein kinase C inhibitors. J. Natl. Cancer Inst. *76*, 1243–1246.

O'Brian, C.A., Housey, G.M., and Weinstein, I.B. (1988a). Specific and direct binding of protein kinase C to an immobilized tamoxifen analogue. Cancer Res. *48*, 3626–3629.

O'Brian, C.A., Ward, N.E., and Anderson, B.W. (1988b). Role of specific interactions between protein kinase C and triphenylethylenes in inhibition of the enzyme. J. Natl. Cancer Inst. *80*, 1628–1633.

Ohshima, T., Ward, J.M., Huh, C.G., Longenecker, G., Veeranna, Pant, H.C., Brady, R.O., Martin, L.J., and Kulkarni, A.B. (1996). Targeted disruption of the cyclin-dependent kinase 5 gene results in abnormal corticogenesis, neuronal pathology and perinatal death. Proc. Natl. Acad. Sci. USA *93*, 11173–11178.

Okada, S., Yamada, E., Saito, T., Ohshima, K., Hashimoto, K., Yamada, M., Uehara, Y., Tsuchiya, T., Shimizu, H., Tatei, K., et al. (2008). CDK5-dependent phosphorylation of the Rho family GTPase TC10(alpha) regulates insulin-stimulated GLUT4 translocation. J. Biol. Chem. *283*, 35455–35463.

O'Neill, K., Chen, S., and Diaz Brinton, R. (2004). Impact of the selective estrogen receptor modulator, tamoxifen, on neuronal outgrowth and survival following toxic insults associated with aging and Alzheimer's disease. Exp. Neurol. *188*, 268–278.

Patrick, G.N., Zukerberg, L., Nikolic, M., de la Monte, S., Dikkes, P., and Tsai, L.H. (1999). Conversion of p35 to p25 deregulates Cdk5 activity and promotes neurodegeneration. Nature *402*, 615–622.

Peterson, D.W., Ando, D.M., Taketa, D.A., Zhou, H., Dahlquist, F.W., and Lew, J. (2010). No difference in kinetics of tau or histone phosphorylation by CDK5/p25 versus CDK5/p35 in vitro. Proc. Natl. Acad. Sci. USA *107*, 2884–2889.

Polychronopoulos, P., Magiatis, P., Skaltsounis, A.L., Myrianthopoulos, V., Mikros, E., Tarricone, A., Musacchio, A., Roe, S.M., Pearl, L., Leost, M., et al. (2004). Structural basis for the synthesis of indirubins as potent and selective inhibitors of glycogen synthase kinase-3 and cyclin-dependent kinases. J. Med. Chem. *47*, 935–946.

Rich, J.N., and Bigner, D.D. (2004). Development of novel targeted therapies in the treatment of malignant glioma. Nat. Rev. Drug Discov. *3*, 430–446.

Sahlgren, C.M., Mikhailov, A., Vaittinen, S., Pallari, H.M., Kalimo, H., Pant, H.C., and Eriksson, J.E. (2003). Cdk5 regulates the organization of Nestin and its association with p35. Mol. Cell. Biol. *23*, 5090–5106.

Smith, D.S., Greer, P.L., and Tsai, L.H. (2001). Cdk5 on the brain. Cell Growth Differ. *12*, 277–283.

Sundaram, J.R., Poore, C.P., Sulaimee, N.H., Pareek, T., Asad, A.B., Rajkumar, R., Cheong, W.F., Wenk, M.R., Dawe, G.S., Chuang, K.H., et al. (2013). Specific inhibition of p25/Cdk5 activity by the Cdk5 inhibitory peptide reduces neurodegeneration in vivo. J. Neurosci. *33*, 334–343.

Tarricone, C., Dhavan, R., Peng, J., Areces, L.B., Tsai, L.H., and Musacchio, A. (2001). Structure and regulation of the CDK5-p25(nck5a) complex. Mol. Cell *8*, 657–669.

Zhang, W., Law, R.E., Hinton, D.R., and Couldwell, W.T. (1997). Inhibition of human malignant glioma cell motility and invasion in vitro by hypericin, a potent protein kinase C inhibitor. Cancer Lett. *120*, 31–38.

Zhang, B., Corbel, C., Gueritte, F., Couturier, C., Bach, S., and Tan, V.B. (2011). An in silico approach for the discovery of CDK5/p25 interaction inhibitors. Biotechnol. J. *6*, 871–881.

